ELSEVIER

Femtosecond studies of crown ethers: supramolecular solvation, local solvent structure and cation–π interaction

Wenyun Lu [a], Weihong Qiu [a], Jongjoo Kim [a], Oseoghaghare Okobiah [a], Jiaxin Hu [b], George W. Gokel [b], Dongping Zhong [a,*]

[a] *Departments of Physics, Chemistry and Biochemistry, OSU Biophysics, Chemical Physics and Biochemistry Programs, The Ohio State University, 174 West 18th Avenue, Columbus, OH 43210, USA*
[b] *Department of Molecular Biology and Pharmacology, School of Medicine, Washington University, 660 South Euclid Avenue, Campus Box 8103, St. Louis, MS 63110, USA*

Abstract

We report here femtosecond studies of microsolvation, host-guest recognition, and cation–π interaction of crown ethers in organic solvents. The side-armed indole ring of the supramolecule acts as an optical probe and a π-donor. Significantly-slow solvation dynamics (e.g. 206 ps in acetonitrile) were observed, revealing ordered local solvent structures. With encapsulation of the alkali-metal cation in the macroring, solvation dynamics become much faster by one order of magnitude, reflecting significant solvent reorganization during molecular recognition. The combined data suggest a folded supramolecular structure involving intercalated solvent molecules or a sandwiched metal cation, consistent with the enhanced local polarization and the strong electrostatic interactions.
© 2004 Elsevier B.V. All rights reserved.

1. Introduction

Crown ethers are heteromacrocycles in which the framework is typically comprised of repeating ethyleneoxy $[-(CH_2CH_2O)_n-]$ units. Nitrogen and sulfur commonly replace oxygen in this framework leading to a great variety of compounds that have been used in molecular recognition studies and supramolecular chemistry [1–6]. Crown ethers form more or less stable complexes in the solution and vapor phases with a variety of organic and metallic cations. In these host-guest recognition processes, solvent plays a critical role in local structure optimization and complex stabilization. Thus, complex stability is known to vary, sometimes drasti-

cally, according to the solvent in which the reaction occurs [7]. Understanding of supramolecule-solvent interactions and structures at the local molecular level is important for potential applications in drug delivery, chemical sensor development, and to supramolecular chemistry in general.

Crown ethers selectively complex various alkali-metal cations and can be thus used as model systems to study interactions between a macrocycle-bound cation and the π-system of a sidearm arene. Alkali-metal cation–π interactions have recently received considerable attention due to the biological importance [6,8–10]. These studies have focused on Na^+ and K^+ interacting with benzene, phenol, and indole, the side chain arenes of phenylalanine, tyrosine, and tryptophan, respectively. Recent work [11–20] has demonstrated the formation of stable complexes between, for example, K^+ and a

---

* Corresponding author. Fax: +1 614 292 7557.
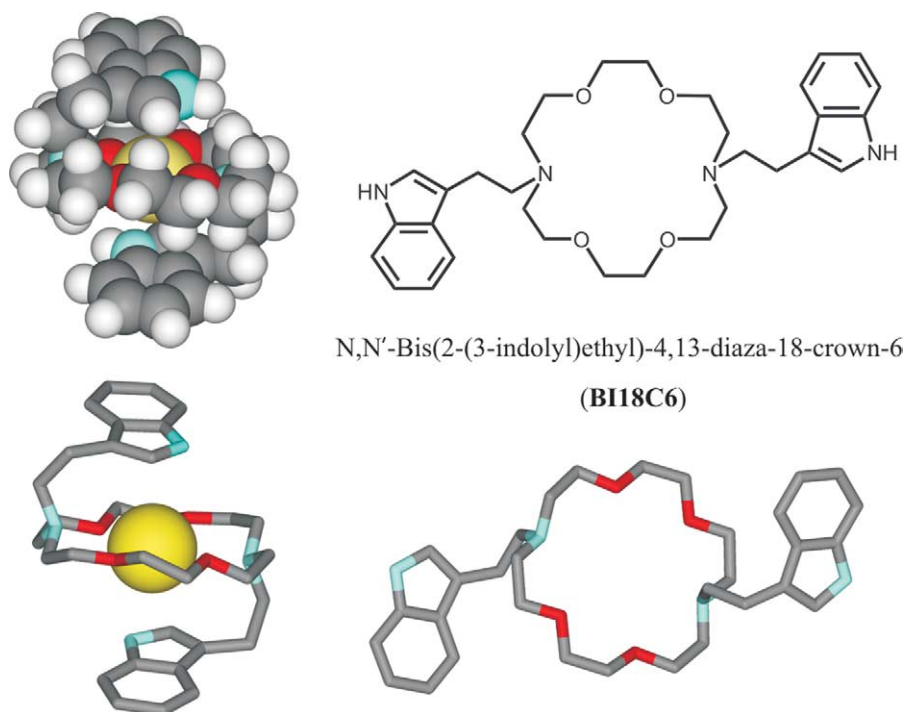*E-mail address:* dongping@mps.ohio-state.edu (D. Zhong).

Fig. 1. Right: Molecular structure of **BI18C6** and its tubular model. Left: The solid-state X-ray structure of compound **BI18C6** complexed with the potassium cation K^+ in CPK and tubular presentations.

crown ether in which two side-armed indole rings are in contact with the macroring-bound cation (see Fig. 1). The complex structure was obtained by the solid-state characterization using X-ray diffraction [12,14,16] and later by NMR studies in solution [11,14].

We report here femtosecond (fs)-resolved studies of two arene side-armed lariat ether receptors in the presence and absence of K^+, in two common solvents: acetonitrile (CH_3CN) and methanol (CH_3OH). The two crown ethers used were *N,N'*-Bis(2-(3-indolyl)ethyl)-4,13-diaza-18-crown-6 (**BI18C6** in Fig. 1, compound **7** in [14]), which has two indolylethyl sidearms, and *N*-(2-(3-indolyl)ethyl)aza-18-crown-6 (compound **9** in [16]), which has a single indolylethyl side chain. The former was chosen as the host supramolecule for study and the latter was studied for comparison. The indole moiety in these molecules was used as an optical probe to examine the solvent relaxation dynamics around the supramolecule with and without encapsulation of K^+. In addition, the corresponding anisotropy was measured for each case. These studies allow us to probe microsolvation around the crown macrorings, to derive certain local solvent structures and to examine cation–π interactions in the crown ether complexes. The results reveal the actual time scales of solvent arrangements in microscopic recognition and provide clear insights concerning the mechanism by which crown ethers recognize metal cations in solution.

2. Experimental

All experiments were done using the fs-resolved fluorescence up-conversion method. The experimental setup has been described elsewhere [21]. Two crown ether compounds used were reported previously [14,18]. A solution of either compound was prepared by dissolving the receptor in either CH_3CN or CH_3OH to a concentration of 2 mM solution. The corresponding cation complexes were obtained by adding KI or KCl until the solution was 20 mM in K^+ ion. The reported binding constants of 18-crown-6 with K^+ are 1.2×10^6 M^{-1} in CH_3OH [13] and 1.3×10^6 M^{-1} in CH_3CN [22], respectively. Binding constants have been measured for *N,N'*-dibenzyldiaza-18-crown-6 in CH_3OH and in CH_3CN for Na^+ but only in the former for K^+. The binding constants are 4.8×10^2 and 2.4×10^3 M^{-1} for Na^+ and K^+ in CH_3OH. In CH_3CN, the Na^+ binding constant was measured as 7.9×10^4 M^{-1} [23]. From these data, we estimated that the K^+ binding constants in CH_3CN and CH_3OH would be at least 10^5 and 10^3 M^{-1}, respectively. Using these binding constants, we obtained 99.9% and 94.8% complexation of **BI18C6** with cations in CH_3CN and CH_3OH, respectively. The complex formation in these solvents is very efficient. For comparison, 5 mM tryptophan solution in CH_3OH was also studied. The solubility of tryptophan in CH_3CN is low, which prevents time-resolved studies.

3. Results and discussion

3.1. Steady-state characterization

All absorption spectra of tryptophan and **BI18C6** in methanol and acetonitrile are similar with an absorption peak of the indole moiety at 281 nm. The steady-state fluorescence spectra obtained using 290 nm excitation are shown in Fig. 2. The corresponding emission maxima are obtained by a log-normal fitting of these spectra. The emission peak of tryptophan in water is at 349 nm [21] and the peak shifts to the blue side at 336.5 nm in methanol and 332.3 nm in acetonitrile, consistent with the decrease trend of dielectric constants. At 25 °C, the dielectric constants of water, methanol and acetonitrile are 80.1, 33.0 and 36.6, respectively [24] and the emission spectra in solvents with lower dielectric constants are usually blue-shifted [25,26].

The emission peak in acetonitrile from the solute tryptophan to **BI18C6** shifts to the red side at 350.5 nm by 1563 cm^{-1}. This observation is striking and quite unusual. The macroring of the crown ether does not significantly change the electronic structures of the indole moiety as also seen in absorption spectra. The observed large shift should be due to the solvent effect; the solvent molecules organize around the macroring of crown ethers and a well-ordered structure is formed, resulting

Fig. 2. Steady-state fluorescence spectra of tryptophan and supramolecule **BI18C6** in CH$_3$CN and CH$_3$OH at excitation of 290 nm. The ball–stick structures of two solvent molecules with their dipole moments are also shown. Note the different shifts in two solvents with and without addition of KI.

in enhancement of the local polarization. With the addition of KI, the emission peak shifts back to the blue side at 340.2 nm. This observation indicates that the supramolecule-solvent structure is probably quite different with and without KI. With the encapsulation of K$^+$, the recognition leads to local solvent rearrangements and thus results in a decrease of the local polarization and a blue shift of the emission. The addition of KCl gave a similar emission maximum at 340.6 nm. In methanol, the emission peak shifts to 344.5 nm by 690 cm^{-1} upon changing tryptophan to **BI18C6**, again reflecting an ordered local solvent structure around the macroring, but with less enhanced local polarization than in acetonitrile. With the addition of KI, the peak slightly shifts to the more red side at 346.4 nm due to the encapsulation of K$^+$. All observed spectral shifts from tryptophan to **BI18C6** are related to ordered supramolecule-solvent structures and solvent dipole moments where acetonitrile is 3.92 Debye (D) while methanol is 1.70 D. The ordered local solvent structures around the crown ether are directly studied by the microsolvation dynamics which are given below.

3.2. Supramolecular solvation dynamics

Fig. 3 shows three typical fs-resolved fluorescence transients of **BI18C6** without and with the addition of KI in acetonitrile from more than ten different gated emissions covering from 305 to 440 nm. All the transients show the typical solvation relaxation behavior with initial decay in the blue-side emission and rise at the red side then followed by the lifetime components. However, with and without encapsulation of K$^+$, the solvation dynamics are drastically different. At 305 nm, the transient without K$^+$ decays with time constants of 0.39 ps (62%), 3.6 ps (8%), 105 ps (13%), and two lifetimes of 500 ps (13%) and 4 ns (4%). With K$^+$, the transient decays with 0.32 ps (72%), 4.6 ps (7%) and two lifetimes of 500 ps (16%) and 3 ns (5%). The long solvation component of 105 ps disappeared by adding KI into the solution. At 330 nm, the transients without K$^+$ can be fitted with decay time constants of 1.35 ps (14%), 11.5 ps (4%), 144 ps (19%), as well as two lifetimes of 500 ps (26%) and 4 ns (37%). With K$^+$ the time constants become 0.98 ps (13%), 18.2 ps (4%), and two lifetimes of 500 ps (38%) and 3 ns (45%). At the far red-side emission of 440 nm, without K$^+$ we observed two rise components with time constants of 0.84 ps (−22%), 261 ps (−41%), and one lifetime decay of 4 ns (100%). With K$^+$, the transient initially rises in 1.2 ps (−36%) followed by the lifetime decay of 3 ns (100%). Clearly, in the absence of KI, one slow solvation component in hundreds of picoseconds appears in all transients, indicating a well-ordered solvent structure around the supramolecule. With encapsulation of K$^+$, this long component is absent in all measured transients, indicative of
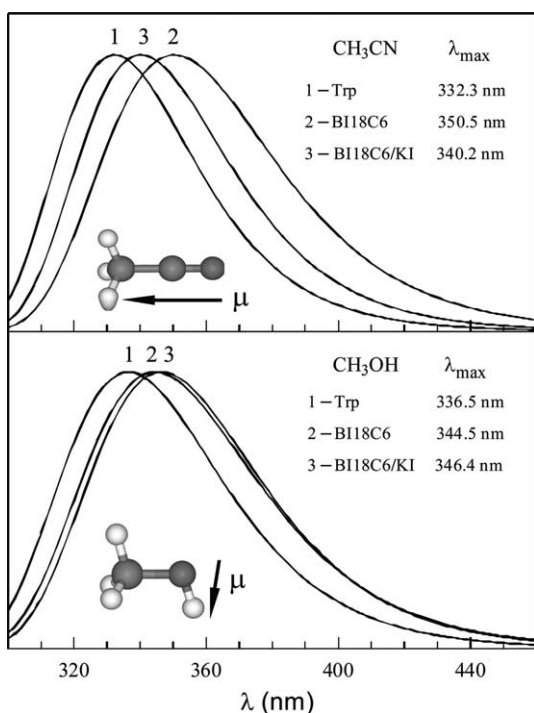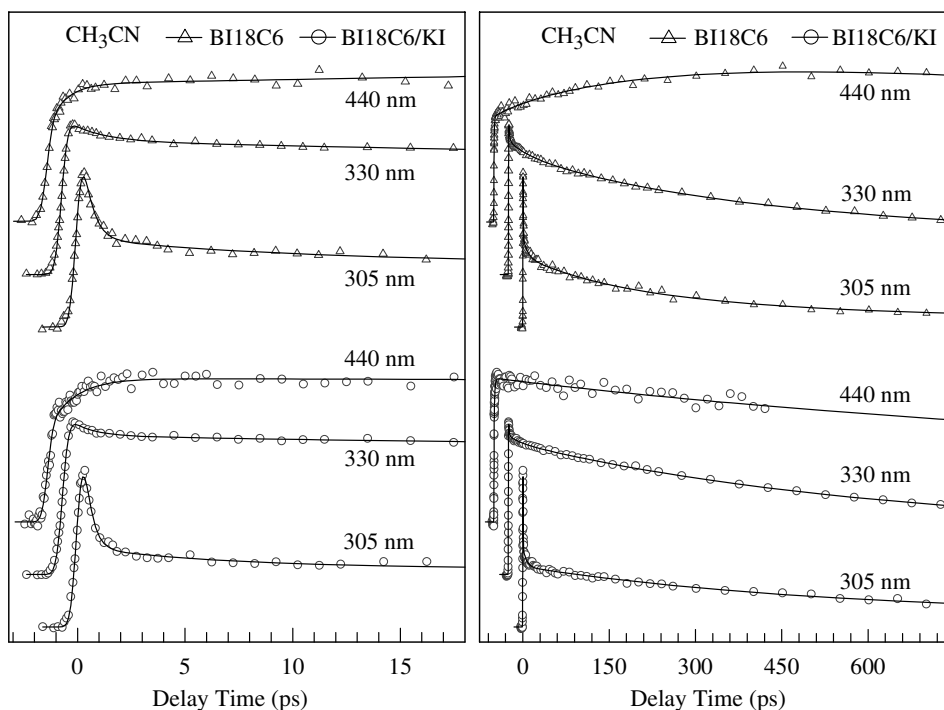
Fig. 3. Normalized, fs-resolved fluorescence transients of the supramolecule **BI18C6** in CH_3CN without and with the addition of KI in the short (left) and long (right) time ranges from more than ten gated fluorescence emissions. Note the drastic difference of transients at the long delay time without and with encapsulation of the cation K^+.

rearrangements of solvent molecules during recognition with a final less ordered structure.

We also systematically measured the fs-resolved fluorescence transients with the addition of KCl and the results are nearly the same as those obtained with KI. The anion Cl^- and I^- make no difference to the solvation dynamics observed here. As a comparison, we also studied another crown ether supramolecule with only one indole sidearm. With and without KI, the results are similar to those obtained for **BI18C6** with two indole sidearms. This observation is consistent with the folded symmetric structure (Fig. 1) and either of two indole rings gives similar solvation behaviors.

We also studied the solvation dynamics of **BI18C6** in CH_3OH. Fig. 4a shows three representative fs-resolved transients from more than ten gated fluorescence emissions. Similarly, all transients in the blue side had two initial exponential decays (0.95–16.3 ps) while in the red side two initial rises (0.55–12 ps) were found, besides the two lifetime contributions. Overall, the solvation dynamics are similar in the presence and absence of K^+ with slightly faster processes for the former. As a comparison, we also examined the solvation dynamics of tryptophan in CH_3OH and the results follow the similar trend.

These fs-resolved fluorescence transients were used to construct the time-resolved fluorescence spectra and then the solvation correlation functions [27]. Using the methodology we recently developed for tryptophan-related systems [21], two series of time-resolved spectra

were calculated for the overall process and the lifetime emission process, respectively and two time-dependent emission maximum curves are produced: One is for the overall process (v_s) and the other for the lifetime emission (v_l). When the two curves merge at the certain time (t_{sc}), we consider that the solvation process has ended. The correlation function is then obtained as follows:

$$c(t) = \frac{v_s(t) - v_l(t)}{v_s(0) - v_l(0)}. \tag{3.1}$$

Fig. 4b shows a series of time-resolved emission spectra of **BI18C6**/KI in methanol and Fig. 4c gives the two constructed time-dependent emission-maximum curves, v_s and v_l. The two curves merge at $29\,240$ cm^{-1} (342 nm) at a time of 120 ps, when the solvation is completed (t_{sc}). The emission spectrum keeps moving to the steady-state emission maximum at 346.4 nm at a time of 1150 ps (t_{ss}). Using Eq. (3.1) we calculated the solvation correlation function and obtained the solvation dynamics. Tables 1 and 2 summarize all analyzed results of the systems studied and Fig. 5a shows the obtained solvation correlation functions.

The solvation correlation function of acetonitrile is best fitted with three exponential decays, 0.48 ps (55%), 3.9 ps (15%) and 206 ps (30%). With the addition of KI, the solvation dynamics are drastically different and become faster with time constants of 0.4 ps (76%), 1.1 (16%), and 21.6 ps (8%). Using KCl instead of KI, the solvation time constants are nearly the same, 0.36
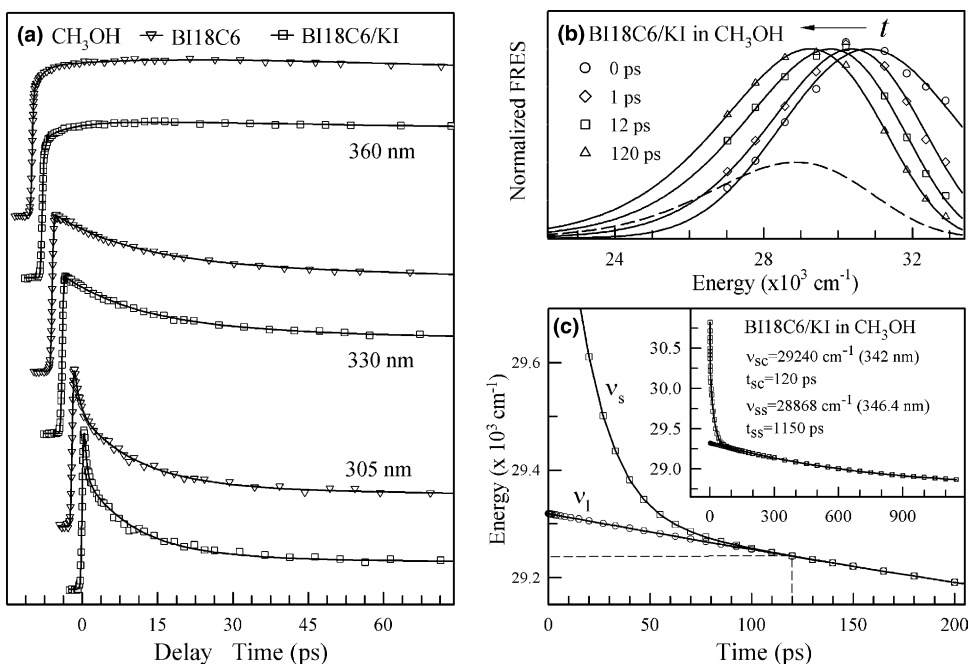
Fig. 4. (a) Normalized, fs-resolved fluorescence transients of the supramolecule **BI18C6** in CH_3OH without and with KI from more than 10 gated fluorescence emissions. (b) Representation of normalized fs-resolved emission spectra (FRES) constructed from (a) at several times for **BI18C6**/KI in CH_3OH. The symbol represents the experimental data and the solid line is a log-normal fit. The dashed line is the steady-state emission spectrum. (c) The fs-resolved emission maxima for the overall process (v_s) and the lifetime emission (v_l). In the insert, the entire evolution of emission maxima for both processes is shown to reach the stead-state emission (v_{ss}); see text.

Table 1
Emission maxima and times from construction of fs-resolved fluorescence spectra[a,b]

	v_0	v_{sc}	t_{sc}	v_{ss}	t_{ss}	v_1	v_2
CH_3CN							
BI18C6	325.17	350.28	1100	350.5	1200	333.1	351.4
BI18C6/KI	321.32	336.55	95	340.2	1250	328.8	341.0
BI18C6/KCl	322.22	337.36	110	340.6	1150	325.4	341.2
CH_3OH							
Tryptophan	315.45	331.82	105	336.5	1150	321.6	337.7
BI18C6	320.90	339.16	130	344.5	1050	332.7	347.5
BI18C6/KI	324.46	342.00	120	346.4	1150	329.7	348.5

[a] v_0, emission maximum at $t = 0$; v_{sc} and t_{sc}, emission maximum and time when solvation ends; v_{ss} and t_{ss}, emission maximum and time when the emission reaches the steady state; v_1 and v_2, emission maxima for the two lifetime components, respectively.

[b] All emission maxima and times are in units of nm and ps, respectively.

ps (74%), 1.2 ps (16%) and 23.4 ps (10%). These results clearly show that the cation has significant effect but the anion is negligible in the supramolecular solvation dynamics. The solvation dynamics of acetonitrile probed by small dye molecules (Coumarin 152 and 153) was reported to be less than 1 ps [28,29]. The solvation dynamics observed here is quite different from that probed by simple dye molecules and contains considerably longer relaxation processes, which must be related to the local solvent structures as discussed in Section 3.3.

For methanol, the solvation correlation function using tryptophan as a probe gives two time constants of 0.39 ps (34%) and 13.3 ps (66%). These results are similar to previous studies [28,29] probed by dye molecules with a slightly longer time constants, which may be due to the different probes. The solvation dynamics probed by the supramolecule **BI18C6** slows down by ~50% but has much less drastic difference than in acetonitrile. These results indicate different ordered local solvent structures around the supramolecule in two solvents. With the addition of KI, the solvation dynamics shows the similar time behavior and suggests no dramatic changes of the local ordered structures before and after recognition.

Table 2
Results obtained for solvation correlation functions[a]

	τ_1	τ_2	τ_3	a_1	a_2	a_3
CH₃CN[b]						
BI18C6	0.48	3.9	206	0.55	0.15	0.30
BI18C6/KI	0.40	1.1	21.6	0.76	0.16	0.08
BI18C6/KCl	0.36	1.2	23.4	0.74	0.16	0.10
CH₃OH[c]						
Tryptophan	0.39	13.3		0.34	0.66	
BI18C6	0.66	17.2		0.29	0.71	
BI18C6/KI	0.58	16.7		0.34	0.66	

[a] All solvation correlation functions are best fitted with $c(t) = \sum_i a_i e^{-t/\tau_i}$ and $\sum_i a_i = 1$. All time constants are in unit of ps.

[b] Previous studies using Coumarin 152 (C152) gave 0.27 ps (73%) and 1.1 ps (27%) [27] and with C153 reported 89 fs (69%) and 630 fs (31%) [28].

[c] Previous studies using C152 gave 1.2 ps (40%) and 9.6 ps (60%) [27] and with C153 reported four components of 30 fs (10%), 280 fs (34%), 3.2 ps (30%) and 15.3 ps (26%) [28].
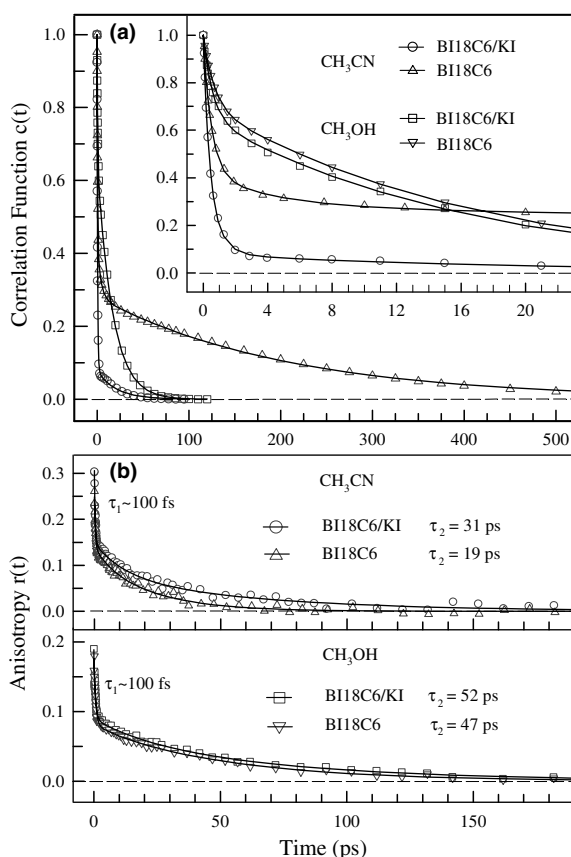

Fig. 5. (a) Solvation correlation functions of CH₃CN and CH₃OH probed by the indole moiety of the supramolecule **BI18C6** with and without encapsulation of the cation K⁺. The inset shows the correlation functions in the short time range. For clarity, the correlation function of CH₃OH probed by **BI18C6** is not shown in the long time range. (b) Femtosecond-resolved anisotropy for the systems studied and note the similar time scales with and without encapsulation of the cation K⁺.

3.3. Local solvent structure, supramolecule recognition and cation–π interaction

The solvation dynamics of acetonitrile probed by the indole moiety of **BI18C6** is drastically different from that of bulk acetonitrile probed by small dye molecules. The difference must result from the local solvent structure around the supramolecule. The observed long solvation time of 206 ps (30%) reflects an ordered solvent structure around **BI18C6** and such slow solvation dynamics have been observed recently for ordered water molecules around protein surfaces [30] and at lipid interfaces [21]. The solid-state structures of **BI18C6** with and without encapsulation of K⁺ have been characterized using X-ray diffraction. Upon the complexation with K⁺, the sidearms of two indole rings fold back onto the macroring with the K⁺ in the center of the ring, forming a folded lariat sandwich structure with two cation–π interactions (Fig. 1). The cation–π interaction was also found to involve with the pyrrolo not the benzo subunit of the indole ring. For **BI18C6** alone, several stretched forms were observed and in these forms the sidearms of two indole rings turn away from each other and no intramolecular interactions were noted between the sidearm and the crown [14,16]. In solution of deuterium acetone, similar structures were observed as in solid phase [11,14].

In acetonitrile, if the supramolecule is in the stretched form, the solvent arrangements around the indole moiety would be similar for both the supramolecule and tryptophan. The resulting solvation dynamics for both molecules would be on the same time scales. The observed long solvation dynamics in the supramolecule indicates a folded structure of **BI18C6**, not stretched, and certain solvent molecules are ordered and sandwiched between the macroring and the indole ring. The CH₃CN has a dipole moment of 3.92 D, much larger than that of H₂O (1.85 D) and CH₃OH (1.70 D). This large dipole moment and the rich negative-charge distributions of both the macroring (four oxygen and two nitrogen atoms) and the indole ring (π electrons) can have large dipole-charge interactions and as a result, the CH₃CN molecules can be well oriented in a mostly parallel-type configuration with the linear C–C–N bonds parallel to two rings. Such parallel-aligned acetonitrile

molecules have been observed recently in pure solution by X-ray diffraction [31]. Thus, the sandwiched solvent molecules are relatively rigid and have direct contacts with both indole rings. The solvent response to the sudden change of the indole dipole moment by electronic excitation is expected to be slow. The ordered local solvent structure results in enhancement of the local polarization, leading to a larger Stokes shift, consistent with the fluorescence emission in Section 3.1.

With the addition of KI, the solvation dynamics drastically changes (Fig. 5a) and becomes much faster. The slow component of 206 ps disappears. This observation suggests that the well-aligned local solvent structure is mostly rearranged. The interactions of the alkali cations with crown ethers such as 18-crown-6 have been studied very well and in all the cases the cation is sitting at the center of the crown ring as a result of cation–oxygen interactions [1–3]. With the addition of the side indole rings, the strong cation–π interactions between K^+ and the two indole sidearms that fold down on the top and bottom of the crown ring have been observed [6]. The bonding energy of the alkali-metal cations with indole is more than 30 kcal/mol [9]. Because of the steric effects and the strong electrostatic interactions, most of the solvent molecules originally sandwiched between the indole and crown ether rings are squeezed out. In this case, the well-aligned solvent structure around the macroring no long exists. On the other side of the indole ring, the indole interacts with mostly bulk acetonitrile molecules, resulting in much faster solvation dynamics which is similar to the results probed by dye molecules. The exclusion of the ordered solvent molecules leads to a decrease of the local polarization and a less Stokes shift; the emission shifts back to the blue side by 10 nm. The observed 20-ps solvation dynamics but with a small 8% amplitude indicates that certain acetonitrile molecules still stick around the complex due to the charged cation and electron-rich crown ring. Experiments on another supramolecule (*N*-(2-(3-indolyl)ethyl)aza-18-crown-6) with only one indole sidearm gave very similar results as for **BI18C6** with and without K^+, consistent with the symmetric folded structure and indicating that the indole ring mainly 'senses' the solvent structure at one side of the macroring.

We also performed time-resolved anisotropy measurements to examine the two similar structures with and without encapsulation of K^+ in CH_3CN (Fig. 5b). In each case, an initial ultrafast component ($\sim$100 fs) was observed and is attributed to the rapid ^1L_b-^1L_a internal conversion [32,33]. For **BI18C6** in CH_3CN, the long component is fitted with a time constant of 19 ps with an amplitude of 0.11. The 19 ps is the complete rotation relaxation time of **BI18C6** in CH_3CN and no noticeable local wobbling motion of the indole ring was observed, indicating a relatively rigid structure, consistent with the folded compact structure. With the addi-

tion of KCl, the time constant slightly increases to 24 ps (not shown), probably indicating a slight increase of the local viscosity by adding the salt. Changing from KCl to KI, the time constant becomes 31 ps and this increase is due to the proximity of the heavy iodine anion to the supramolecule. The X-ray study revealed a hydrogen bonding between I^- and the nitrogen of the indole ring [16]. On the other hand, if the **BI18C6** in CH_3CN adopts a stretched form, this form would have a very different molecular volume from the folded structure. Using the Stokes–Einstein–Debye hydrodynamics theory [34], the complete rotation relaxation of the stretched structure takes a longer time than the folded form at least by a factor of three but we observed a similar time. This observation suggests a similar structure, consistent with the solvation studies.

In methanol, the complete rotation relaxation with and without K^+ takes a similar time, 52 and 47 ps, respectively (Fig. 5b). A similar folded structure is expected for **BI18C6**. This folded structure with certain oriented methanol molecules results in the 8-nm fluorescence Stokes shift to the red side and the observed slower solvation dynamics. The dipole moment of methanol is small (1.7 D) and methanol molecules form hydrogen-bonding structures. Thus, the local structure of methanol around the macroring is less ordered than that of acetonitrile and the local polarization is less enhanced.

The dynamic process of the cation recognition by the supramolecule crown ether is governed by free energy evolution of total enthalpy and entropy. The desolvation of the cation solvent shell and destruction of the local solvent structure of the host supramolecule are unfavorable in energy but they are compensated by the large energy stabilization through the two strong cation–π (indole) and four cation–oxygen (crown ring) interactions. The solvation dynamics around the K^+ cation is at most as slow as tens of picoseconds [35]. Clearly, in acetonitrile the deconstruction of local solvent structures is the rate-limiting step to reach the final recognition while in methanol both desolvation processes of the cation and the macroring are critical to molecular recognition because they occur on the similar time scale. The strong electrostatic interactions of the cation with the electron-rich indole π-rings and oxygen atoms are the dominant recognition force and control the entire recognition process.

4. Conclusion

In this contribution, by using the side-armed indole ring as an optical probe as well as a π-donor, we studied with femtosecond resolution the microsolvation, host-guest recognition and cation–π interaction of the supramolecule crown ether in acetonitrile and methanol. The

observed slow microsolvation dynamics reveals a highly ordered local solvent structure around the crown ether, which results in enhancement of the local polarization and thus the large solvent stabilization energy (large Stokes shift in emission). Molecules can have large stabilization energy but with slow solvation dynamics as we observed here in acetonitrile and also in ordered water at lipid interfaces [21]. With encapsulation of the alkali-metal cation, the solvation dynamics becomes much faster by one order of magnitude, reflecting significant solvent reorganization during molecular recognition. The femtosecond-resolved anisotropy measurements revealed similar rotation relaxation dynamics with and without complexation of the alkali-metal cation. These results suggest a folded supramolecular structure with each indole-ring above and below the macroring. The solvent molecules intercalate between the indole and crown-ether rings through the strong dipole-negative charge interactions while in the recognition complex the cation 'squeezes' out the solvent molecules and is finally hosted at the center of the macroring and sandwiched between two indole rings through the strong positive-negative charge attractions.

Acknowledgements

References

[1] J.-M. Lehn, Angew. Chem. Int. Ed. 27 (1988) 89.
[2] D.J. Cram, Angew. Chem. Int. Ed. 27 (1988) 1009.
[3] C.J. Pedersen, Angew. Chem. Int. Ed. 27 (1988) 1021.
[4] G.W. Gokel, Crown Ethers and Cryptands, Royal Society of Chemistry, Cambridge, 1991.
[5] J.A. Semlyen (Ed.), Large Ring Molecules, Wiley, Chichester, 1996.
[6] G.W. Gokel, W.M. Leevy, M.E. Weber, Chem. Rev. 104 (2004) 2723.
[7] R.M. Izatt, K. Pawlak, J.S. Bradshaw, R.L. Bruening, Chem. Rev. 91 (1991) 1721 reference therein.
[8] D.A. Dougherty, Science 271 (1996) 163.
[9] J.C. Ma, D.A. Dougherty, Chem. Rev. 97 (1997) 1303.
[10] E.A. Meyer, R.K. Castellano, F. Diederich, Angew. Chem. Int. Ed. 42 (2003) 1210.
[11] S.L. De Wall, E.S. Meadows, L.J. Barbour, G.W. Gokel, J. Am. Chem. Soc. 121 (1999) 5613.
[12] S.L. De Wall, E.S. Meadows, L.J. Barbour, G.W. Gokel, Proc. Nat. Acad. Sci. USA 97 (2000) 6271.
[13] G.W. Gokel, S.L. De Wall, E.S. Meadows, Eur. J. Org. Chem. (2000) 2967.
[14] E.S. Meadows, S.L. De Wall, L.J. Barbour, G.W. Gokel, J. Am. Chem. Soc. 123 (2001) 3092.
[15] G.W. Gokel, L.J. Barbour, S.L. De Wall, E.S. Meadows, Coord. Chem. Rev. 222 (2001) 127.
[16] J.X. Hu, L.J. Barbour, G.W. Gokel, Proc. Natl. Acad. Sci. USA 99 (2002) 5121.
[17] G.W. Gokel, L.J. Barbour, R. Ferdani, J.X. Hu, Acc. Chem. Res. 35 (2002) 878.
[18] J.X. Hu, L.J. Barbour, G.W. Gokel, J. Am. Chem. Soc. 124 (2002) 10940.
[19] J.X. Hu, L.J. Barbour, R. Ferdani, G.W. Gokel, Chem. Comm. (2002) 1810.
[20] G.W. Gokel, Chem. Comm. (2003) 2847.
[21] W. Lu, J. Kim, W. Qiu, D. Zhong, Chem. Phys. Lett. 388 (2004) 120.
[22] A.F. Danil de Namor, M.L. Zapata-Ormachea, O. Jafou, N. Al Rawi, J. Phys. Chem. B 101 (1997) 6772.
[23] D.A. Gustowski, V.J. Gatto, J. Mallen, L. Echegoyen, G.W. Gokel, J. Org. Chem. 52 (1987) 5172.
[24] D.R. Lide (Ed.), CRC Handbook of Chemistry and Physics, 84th ed., CRC Press, Florida, 2003.
[25] J. Malicka, M. Groth, J. Karolczak, C. Czaplewski, A. Liwo, W. Wiczk, Biopolymers 58 (2001) 447.
[26] C. Reichardt, Solvents and Solvent Effects in Organic Chemistry, third ed., Wiley, Weinheim, 2003.
[27] M. Maroncelli, G.R. Fleming, J. Chem. Phys. 86 (1987) 6221.
[28] W. Jarzeba, G.C. Walker, A.E. Johnson, P.F. Barbara, Chem. Phys. 152 (1991) 57.
[29] M.L. Horng, J.A. Gardecki, A. Papazyan, M. Maroncelli, J. Chem. Phys. 99 (1995) 17311.
[30] S.K. Pal, A.H. Zewail, Chem. Rev. 104 (2004) 2099.
[31] T. Takamuku, M. Tabata, A. Yamaguchi, J. Nishimoto, M. Kumamoto, H. Wakita, T. Yamaguchi, J. Phys. Chem. B 102 (1998) 8880.
[32] D. Zhong, S.K. Pal, D. Zhang, S.I. Chan, A.H. Zewail, Proc. Nat. Acad. Sci. USA 99 (2002) 13.
[33] X. Shen, J.R. Knutson, J. Phys. Chem. B 105 (2001) 6260.
[34] J.S. Baskin, M. Chachisvilis, M. Gupta, A.H. Zewail, J. Phys. Chem. A 102 (1998) 4158.
[35] W. Lu, D. Zhong, J. Phys. Chem. B, in preparation.